DNA as a one-dimensional chiral material. II. Dynamics of the structural transition between B form and Z form

Teruaki Okushima* and Hiroshi Kuratsuji
Research Organization of Science & Engineering, Ritsumeikan University, Noji-higashi 1-1-1, Kusatsu 525-8577, Japan
(Received 29 July 2012; published 8 October 2012)

We analyze the dynamics of structural transitions between normal right-handed B form and unusual left-handed Z form for a linear DNA molecule. The dynamics under the external torque in physiological buffer is modeled by a Langevin equation, with the potential term given by the authors previously [Phys. Rev. E **84**, 021926 (2011)]. With this model, we first simulate the relaxation processes around B-form structure after sudden changes of the external torques, where slow relaxation $\sim t^{-1/2}$ as a function of the elapsed time t is observed. Then, the dynamics of structural transition from Z form to B form is computed under various external torque strength. For small external torques, the transition proceeds via nucleation and the growth, while for higher torques, Z-form structure becomes unstable, and the transition mechanism is switched to a spinodal-like process. These numerical results are qualitatively understood by simple phenomenological arguments.

DOI: 10.1103/PhysRevE.86.041905 PACS number(s): 87.14.gk, 82.37.Rs, 87.15.hp

I. INTRODUCTION

Recent advances in experimental techniques shed light on the response of single double-stranded DNA molecules to mechanical stresses, such as twisting and stretching [1–3]. Various theoretical models have been developed to describe the mechanical responses of the molecule. For example, an extended theory of the classic elastic rod model can describe the supercoiling and its statistical properties [3–8]. Statistical models that phenomenologically describe various structural transitions were developed in Ref. [9]. Several mesoscopic models have also been developed, which can describe the interaction between DNA conformation and *melting* structural transition [10,11]. In our previous paper [12], guided by a gauge principle, we have developed a mesoscopic model of DNA that describes the interplay between the global configuration and the various intrinsic structures of DNA base pairs, such as B and Z structures. In Ref. [12], we have also constructed an effective potential that describes B-Z transition of GC base-pair repeats and elucidated the statistical properties that the GC repeats tend to make structural transition between the usual right-handed B form and unusual left-handed Z form under small external torques, in agreement with the recent experiment of Lee *et al.* [13]. The GC repeats are frequently included in DNA sequences of promoter regions, and furthermore, in recent studies [14], the Z-form structure is related to genetic instability.

In this paper we are concerned with the B-Z transition dynamics. To construct the dynamical model, we first consider the Lagrangian for the linear DNA molecule by introducing kinetic energy, in addition to the effective potential energy given in Ref. [12]. From this Lagrangian, the Euler-Lagrange equations of motions are derived. To model the effect of surrounding physiological buffer, we moreover include viscous torques and random forces into the equations of motions. The resulting equations of motion are utilized to analyze both the relaxation dynamics and the B-Z transition dynamics under various external torques. An alternative approach to B-Z transition was proposed in Ref. [15], where the structural transition dynamics for an idealized dissipationless DNA molecule were mediated by uniformly moving kinks. (See the Appendix for the application of the alternative treatment to our model.) However, as we see below, the viscosity of the surrounding solution completely alters the transition mechanism. In particular, the transition mechanism is switched from a statistically homogeneous nucleation process to a spatially inhomogeneous spinodal-like dynamically unstable process, as the external torque is increased.

II. FORMULATION

In the following, we introduce a nonlinear dynamical model that is a generalization of the static model given in Ref. [12]. To this end, we first construct the Lagrangian of a *linear* DNA molecule. The total potential energy is a functional of torsional angle of sugar-phosphate backbones $\chi(s)$ and structural order parameter $\rho(s)$, where s is the continuous parameter representing the number of bases from one end of the molecule. The potential energy density is given by

$$\mathcal{F} = \frac{C}{2}\left(\frac{d\chi}{ds} - \rho\right)^2 + \frac{d_1}{2}\left(\frac{d\rho}{ds}\right)^2 + \mathcal{V}(\rho), \tag{1}$$

where $C = 91 \times 10^{-20}\mathrm{J}, d_1 = D_1/\omega_0^2$ with $D_1 = 4.1 \times 10^{-21}\mathrm{J}$, and $\omega_0 = 0.6$ rad/bp [12]. The potential density $\mathcal{V}(\rho)$ is given by

$$\mathcal{V}(\rho) = \mathcal{V}_0[(\rho/\omega_0)^2 - 1]^2 + \tau_c\rho, \tag{2}$$

with $\tau_c = -7.9 \times 10^{-21}$ Nm [16] and $\mathcal{V}_0 = 6 \times 10^{-20}\mathrm{J}$, where the B-DNA and Z-DNA conformations correspond to the minima at around $\rho = \omega_0$ and $\rho = -\omega_0$, respectively. These parameter values are given in Ref. [12] to reproduce thermal equilibrium properties.

The structural order parameter $\rho(s)$ is related to the base-pair torsion, namely, the angle $\Theta(s)$ subtended at the center axis of linear DNA, as

$$\frac{d\Theta(s)}{ds} = \rho(s).$$

*okushima@ike-dyn.ritsumei.ac.jp

Now, besides the potential energy (1), we shall take account of the kinetic energy terms coming from the angular variables Θ and χ. These are introduced in the following manner: The first is concerning Θ. The inertia moment of a base pair I_1 is estimated as a rigid rod of length $L = 2$ nm ($\simeq$the diameter of DNA), approximately given by

$$I_1 = \frac{M_1 L^2}{12} = 1.47 \times 10^{-43}\ \text{kg m}^2,$$

where M_1 is the total mass of a GC base pair, 262.228 g/mol $= 4.4 \times 10^{-25}$ kg, which is estimated as the sum of the masses of bases G and C (151.126 and 111.102 g/mol, respectively). Using these, the kinetic energy of base pairs is given by

$$\mathcal{K}_1 = \frac{I_1}{2}\left(\frac{d\Theta}{dt}\right)^2.$$

The second is concerning χ. The inertia of moment for sugar-phosphate backbone chain I_2 is similarly given by

$$I_2 = M_2 \times (1\text{nm})^2 = 7.8 \times 10^{-43}\ \text{kg m}^2,$$

where M_2 is the mass of backbone chain per bp given by $M_2 = 3.9 \times 10^{-25}$ kg, which is estimated as the sum of two deoxyriboses (2×134.13 g/mol) and two phosphoric acids (2×98 g/mol). Then, the kinetic energy of sugar-phosphate backbone per bp is given by

$$\mathcal{K}_2 = \frac{I_2}{2}\left(\frac{d\chi}{dt}\right)^2.$$

In single-molecule experiments, one end of a DNA molecule is fixed to a surface and thus, without loss of generosity, we impose the following condition at the end of $s = 0$:

$$\Theta(0) = \chi(0) = 0.$$

Furthermore, suppose that the external torque τ is exerted on the other end $s = N$, where N is the total bp length of the DNA molecule. Hence, the following potential is added to the Lagrangian:

$$V_{\text{ext}} = -\tau\chi(N).$$

Putting all terms together, the total Lagrangian is given by

$$\begin{aligned} L &= \int_{s=0}^{N} (\mathcal{K}_1 + \mathcal{K}_2 - \mathcal{F})ds - V_{\text{ext}} \\ &\equiv K_1 + K_2 + F - V_{\text{ext}}. \end{aligned} \tag{3}$$

For the sake of the numerical implementation, we discretize the argument s of dynamical variables $\rho(s,t)$ and $\chi(s,t)$, into $s = 0, ds, 2ds, \ldots, nds(= N)$. Then, using $\Theta_0 = 0$, we have

$$\Theta_i(t) = \sum_{j=1}^{i} \rho_j(t)\, ds$$

and

$$\frac{d}{dt}\Theta_i(t) = \sum_{j=1}^{i} \dot{\rho}_j(t)\, ds.$$

Accordingly, $K_1 = \int_0^n \mathcal{K}_1\, ds$ is given by

$$K_1 = \frac{I_1}{2}\, ds^3 \sum_{i=1}^{n}\left[\sum_{j=1}^{i}\dot{\rho}_j(t)\right]^2.$$

Similarly, we obtain the following discretized expressions for K_2 and F, respectively:

$$K_2 = \frac{I_2}{2}\, ds \sum_{i=1}^{n} \dot{\chi}_i^2(t), \tag{4}$$

$$\begin{aligned} F = {} & \frac{C}{2}\, ds \sum_{i=1}^{n}\left(\frac{\chi_i - \chi_{i-1}}{ds} - \rho_i\right)^2 \\ & + \frac{d_1}{2}\sum_{i=1}^{n-1}\frac{(\rho_{i+1} - \rho_i)^2}{ds} + \sum_{i=1}^{n} ds\,\mathcal{V}(\rho_i). \end{aligned} \tag{5}$$

The Euler-Lagrange equation $\frac{d}{dt}\frac{\partial K_1}{\partial \dot{\rho}_i} = -\frac{\partial F}{\partial \rho_i}$ gives the equation of motion for ρ_j:

$$I_1\, ds^3 \sum_{k=i}^{n}\sum_{j=1}^{k}\ddot{\rho}_j(t) = f_i, \tag{6}$$

where $f_i = -\partial F/\partial\rho_i$ is given by

$$\begin{aligned} f_i = {} & C\, ds\left(\frac{\chi_i - \chi_{i-1}}{ds} - \rho_i\right) - d_1\, ds\frac{2\rho_i - \rho_{i-1} - \rho_{i+1}}{ds^2} \\ & - ds\,\mathcal{V}'(\rho_i). \end{aligned} \tag{7}$$

Similarly, from the Euler-Lagrange equation for χ_i, one obtains the following equation of motion for χ_i:

$$I_2\, ds\,\ddot{\chi}_i = g_i,$$

where $g_i = -\partial F/\partial\chi_i$ is given by

$$\begin{aligned} g_i = {} & -C\, ds\left[\frac{\rho_{i+1} - \rho_i}{ds} - \left(\frac{\chi_{i+1} - \chi_i}{ds^2} - \frac{\chi_i - \chi_{i-1}}{ds^2}\right)\right] \\ & + \tau\delta_{i,n}. \end{aligned} \tag{8}$$

Now we model the solvent effect to the DNA molecule by a Langevin equation. For simplicity, here we neglect the hydrodynamic long-range interactions between DNA segments, which would be important especially for curved, long DNA molecules. The Reynolds number (=inertial force/viscous force) is so small in this situation that the viscous forces and thermal random forces thermally equilibrate the DNA molecule. Then the viscous force is estimated as follows. When a segment of sth bp rotates at angular velocity $\omega = d\chi/dt$, the solvent sticks to the DNA surface, and the specific speed of fluid flow is $v \sim \omega R$, where R is the radius of DNA. Hence, we obtain the velocity gradient $\sim\omega R/R = \omega$, and the corresponding shear stress $\sim\eta\omega$, where η is the viscosity coefficient. In the following, the values of water (1 mPa s) is used for η. The viscous forces applied to the DNA segment is given by $\kappa A\eta\omega$, where A is the area of the DNA side surface and a dimensionless coefficient κ is introduced. For simplicity, A is approximated by $2\pi Rh$, i.e., the area of side surface of cylinder with the radius R of DNA ($\sim$1 nm) and the height h of the 1 bp DNA segment($\sim$ 0.34 nm). Then the viscous torque

is given by

$$\begin{aligned}&(\text{viscous force}) \times R \\ &= 2\pi\kappa R^2 h\eta\omega \sim 2.14\kappa \times 10^{-30}\,\text{kg m}^2/\text{s} \times \omega \equiv \kappa\alpha\omega. \quad (9)\end{aligned}$$

Hence, the equation of motion for χ_i is modified as

$$I_2\, ds \frac{d^2\chi_i}{dt^2} = g_i - \kappa\alpha\, ds \frac{d\chi}{dt} + \xi_i(t). \quad (10)$$

Here the random forces $\xi_i(t)$ are introduced as Gaussian white processes satisfying

$$\langle \xi_i(t)\xi_j(0)\rangle = 2\kappa\alpha\, ds \times k_B T\delta(t)\delta_{ij}, \quad (11)$$

where k_B is the Boltzmann constant and T is the temperature of the surrounding buffer. Note that Eqs. (10) and (11) guarantee the ith segment's rotational energy $I_2 ds\dot{\chi}(t)^2/2$ to reach the thermal value at temperature T. Moreover, we postulate that the buffer does not affect the dynamics of ρ, because, in B form or Z form, base pairs are located inside the DNA molecule and apart from the buffer.

In the limit of $ds \to 0$, one obtains the following coupled stochastic partial differential equations:

$$\begin{aligned}&I_1 \int_{s_2=s}^{n}\int_{s_1=0}^{s_2} \frac{\partial^2\rho(s_1,t)}{\partial t^2}\, ds_1\, ds_2 \\ &= C\left[\frac{\partial\chi(s,t)}{\partial s} - \rho(s,t)\right] - \mathcal{V}'[\rho(s,t)] + d_1\frac{\partial^2\rho(s,t)}{\partial s^2} \quad (12)\end{aligned}$$

and

$$\begin{aligned}I_2\frac{\partial^2\chi(s,t)}{\partial t^2} &= C\left[\frac{\partial^2\chi(s,t)}{\partial s^2} - \frac{\partial\rho(s,t)}{\partial s}\right] \\ &\quad -\kappa\alpha\frac{\partial\chi(s,t)}{\partial t} + \tilde{\xi}(s,t) + \tau\delta(s-N), \quad (13)\end{aligned}$$

where $\tilde{\xi}(i\ ds,t) = \xi_i/ds$ is scaled random noise satisfying

$$\langle\tilde{\xi}(s_1,t_1)\tilde{\xi}(s_2,t_2)\rangle = 2\kappa\alpha k_B T\delta(s_1 - s_2, t_1 - t_2).$$

Note here that, in the $ds \to 0$ limit with $\kappa = 0$ and $T = 0$, the resulting coupled wave equations for Θ and χ are formally equivalent to the model of Volkov [17,18]. These equations have a kink solution, as a special solution, whose detailed derivation is given in the Appendix.

III. NUMERICAL METHOD

In this section, we develop the numerical method for solving (6) and (10). In the following, we set $ds = 1$ for simplicity.

First, dimensionless variables are introduced by measuring energy in units of $\mathcal{V}_0$ and time in units of $\sqrt{I_1/\mathcal{V}_0}(= 1.5625 \times 10^{-12}\,\text{s})$. These equations read:

$$\begin{aligned}&\sum_{k=i}^{n}\sum_{j=1}^{k}\frac{d^2\rho_j(t)}{dt^{*2}} \\ &= C^*(\chi_i - \chi_{i-1} - \rho_i) + d_1^*(2\rho_i - \rho_{i-1} - \rho_{i+1}) \\ &\quad - 4[(\rho/\omega_0)^2 - 1]\rho/\omega_0 + \tau_c^* \quad (14)\end{aligned}$$

and

$$\begin{aligned}I_2^*\frac{d^2\chi_i}{dt^{*2}} &= -C^*[\rho_{i+1} - \rho_i - (\chi_{i+1} - \chi_i - \chi_i - \chi_{i-1})] \\ &\quad -\kappa\alpha^*\frac{d\chi}{dt^*} + \xi_i(t^*) + \tau_{i,n}^*, \quad (15)\end{aligned}$$

where the asterisks denote dimensionless quantities: $C^* = C/\mathcal{V}_0$, $d_1^* = d_1/\mathcal{V}_0$, $\tau_c^* = \tau_c/\mathcal{V}_0$, $\tau^* = \tau/\mathcal{V}_0$, $I_2^* = I_2/I_1$, and $\alpha^* = \alpha/\sqrt{I_1\mathcal{V}_0}$. Random forces $\xi_i(t^*)$ satisfy

$$\langle\xi_i(t_1^*)\xi_j(t_2^*)\rangle = 2\kappa\alpha^* T^*\delta(t_1^* - t_2^*)\delta_{ij},$$

where the dimensionless temperature T^* is introduced as

$$T^* = k_B T/\mathcal{V}_0 \qquad (= 0.07 \text{ at } 300\text{ K}). \quad (16)$$

In the computation of Eq. (14), it must be solved for $\ddot{\rho}_i = \partial^2\rho_i/\partial t^{*2}$. Denoting the right-hand side of Eq. (14) by f_i^*, we rewrite (14) as

$$\sum_{j=1}^{i}\ddot{\rho}_j + \sum_{k=i+1}^{n}\sum_{j=1}^{k}\ddot{\rho}_j = f_i^*.$$

Hence,

$$\sum_{j=1}^{i}\ddot{\rho}_j = f_i^* - f_{i+1}^* \equiv \delta f_i^*.$$

We again rewrite this equation as

$$\ddot{\rho}_i + \sum_{j=1}^{i-1}\ddot{\rho}_j = \delta f_i^*$$

and obtain the following result:

$$\ddot{\rho}_i = \delta f_i^* - \delta f_{i-1}^* \equiv \delta^2 f_i^*. \quad (17)$$

In our computation, Eqs. (15) and (17) are numerically integrated. At every dt-time-step computation, each random force in Eq. (15) is set as $\xi_i dt = R$, where R is a random number sampled from the Gaussian distribution with mean zero and variance $\sqrt{2\kappa\alpha^* T^* dt}$.

IV. DYNAMICS OF A LINEAR DNA MOLECULE

A. Slow relaxation

Here we study the relaxation after a sudden change of external torque. To begin, we estimate two specific time scales: relaxation time and oscillation period. The specific relaxation time is given by

$$t_{\text{relax}} \equiv \frac{I_2}{\kappa\alpha} = 3.6\kappa^{-1} \times 10^{-13}\,\text{s} = 0.23\kappa^{-1}\sqrt{I_1/\mathcal{V}_0},$$

while the time scale of oscillation is

$$t_{\text{osc}} \equiv \sqrt{\frac{I_2}{C}} = 9.258 \times 10^{-13} \times 10^{-12}\,\text{s} = 0.6\sqrt{I_1/\mathcal{V}_0}.$$

Then, at first, one might expect that the dynamics were classified into two: overdamped dynamics if $\kappa > 1/3.6 \sim 0.27$ and underdamped dynamics if $\kappa < 1/3.6 \sim 0.27$. However, as we shall see below, the dynamics show more complicated, slow relaxations $\propto t^{-1/2}$, where the relaxation time t_{relax} will turn out to be the key factor for determining the prefactor of the slow relaxations. Hereafter, we use dimensionless quantities and

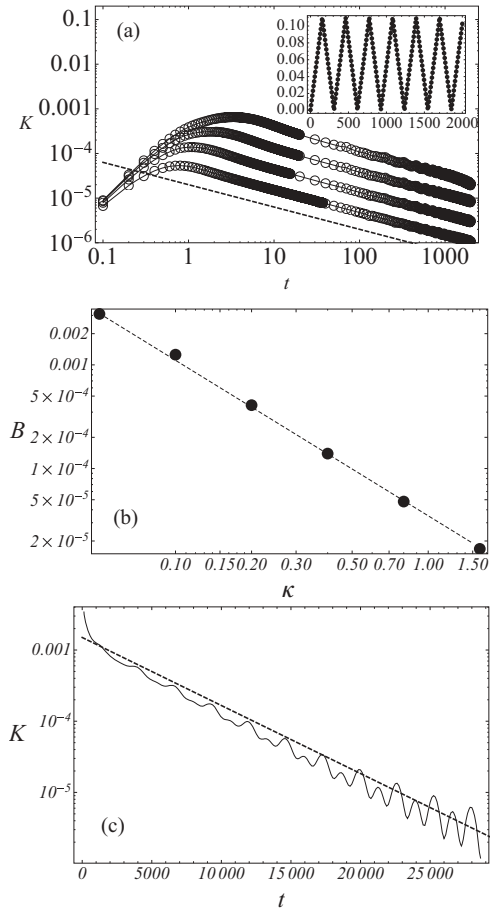

FIG. 1. (a) Total kinetic energies K are plotted as functions of time t after sudden addition of external torque $\tau = 1$, for $\kappa = 0.1, 0.2, 0.4, 0.8$ from top to bottom. The dashed line $\propto t^{-0.5}$ is drawn for eye guidance. Long-time dynamics of K for various κ show slow relaxations $B(\kappa)t^{-1/2}$. (Inset) K vs t for the conserved system ($\kappa = 0$). (b) Plot of coefficient B as a function of κ. The values of B are obtained by fitting the data of $t > 10$ in Fig. (a) to $Bt^{-0.5}$. The dashed line is $0.000035\kappa^{-3/2}$, which clearly shows $B \sim \kappa^{-3/2}$. (c) Semilog plot of K vs t for the linearized system near $\rho = \omega_0$ with $\kappa = 0.2$ and $\tau = 1$. The dashed line $\propto e^{-0.00022t}$ shows the exponential decay.

omit, for the sake of notational simplicity, the asterisks on the symbols.

We simulated the relaxation dynamics at $T = 0$. The initial state was prepared as B-form structure, namely,

$$\rho_i = \omega_0, \quad \chi_i = \omega_0 i \quad \text{for} \quad i = 1,2,\ldots,n,$$

where $ds = 1$ and the length of the DNA was set as $n = 200$. At $t > 0$, the external torque of $\tau = 1$ was suddenly exerted on the nth bp segment. We computed how the DNA state relaxed to a new stable state of twisted B-form structure for various dimensionless dissipation coefficients κ.

Figure 1(a) shows the total kinetic energies $K = K_1 + K_2$ as functions of time for various κ. For all κ computed, there are slow relaxations $B(\kappa)t^{-1/2}$, at their late times. The prefactor $B(\kappa)$ is plotted in Fig. 1(b), as a function of κ. We clearly see the relation $B(\kappa) \propto \kappa^{-3/2}$ holds. This is qualitatively understood as follows: As shown in the inset of Fig. 1(a), $K \propto t$ ($t < 100$) for the conserved system of $\kappa = 0$. Then the nonconservative systems of $\kappa \neq 0$ would depart from the behavior of the conserved system at the relaxation times t_{relax}. At the times, the kinetic energy K would also have their maximum values $K \propto t_{\text{relax}} \sim \kappa^{-1}$. After the times, K show slow relaxation $K \propto t^{-1/2}$. Putting these estimates together, the following relation is derived:

$$K \sim \kappa^{-1} \left(\frac{t}{t_{\text{relax}}} \right)^{-1/2} \sim \kappa^{-3/2} t^{-1/2}.$$

This qualitatively agrees with the above mentioned numerical result: $B(\kappa) \propto \kappa^{-3/2}$.

Notice that the relaxations studied here are not usual exponential but an anomalously slow one $\sim t^{-1/2}$. This type of slow relaxation is well known in the studies on one-dimensional nonlinear dynamical systems (e.g., Ref. [19]). For comparison, the torque response of the linearized equations near $\rho = \omega_0$ is plotted in Fig. 1(c), from which we see that K relaxes exponentially with t. Hence, the origin of the observed power-law relaxation dynamics is the nonlinear coupling in quasi-one-dimensional DNA molecules.

B. Transition from Z form to B form

Now we consider the dynamics of structural transition from Z form to B form.

The initial state was prepared as Z-form structure, namely,

$$\rho_i = -\omega_0, \quad \chi_i = -\omega_0 i \quad \text{for} \quad i = 1,2,\ldots,n,$$

where the length of the DNA was set as $n = 200$. At $t > 0$, the external torque $\tau \geqslant 0$ was suddenly exerted on the nth bp segment. We computed how the DNA state relaxed to the stable B-form structure from the initial Z-form structure, at the room temperature $T = 0.07$ [see Eq. (16)].

The transition dynamics from Z form to B form is shown in Fig. 2(a)–2(b), for $\tau = 0$ and $\kappa = 0.01$. From Fig. 2(a), we clearly see the following: (1) The stable B-form domains, indicated in light gray in the figure, are quickly created from the beginning of time evolution. (2) Then, the mixed states of B-form and Z-form structures are formed, where the statistical weights of B form grow in the course of time evolution. (3) Eventually, almost all segments become B-form structures. Note here that, if the nucleation is a random process with probability p, the frequency of domain size D should scale as $\propto p^D$. Figure 2(b) shows that this scaling relation indeed holds for B domains larger than two segments and that the critical size of the nucleation is two segments. As a result of the statistically uniform nucleation, χ_i changes with keeping the linear shape $\chi_i \propto i$ [Fig. 2(c)]. More preciously, the following approximate relation holds:

$$\chi_i \simeq i\langle\rho\rangle + \text{fluctuating term},$$

where $\langle\rho\rangle$ denotes the average value of ρ_i. This is easily understood because $\chi_i \simeq \sum_{j=1}^{i} \rho_j$ holds and because one can replace ρ_j in this equation by $\langle\rho\rangle$ for the statistically uniform nucleations.

Now we consider how the nucleation rate depends on the external torque strength. When a small torque is exerted on a terminal, the interactions between neighboring segments will quickly induce torque balances on all the segments. Then the

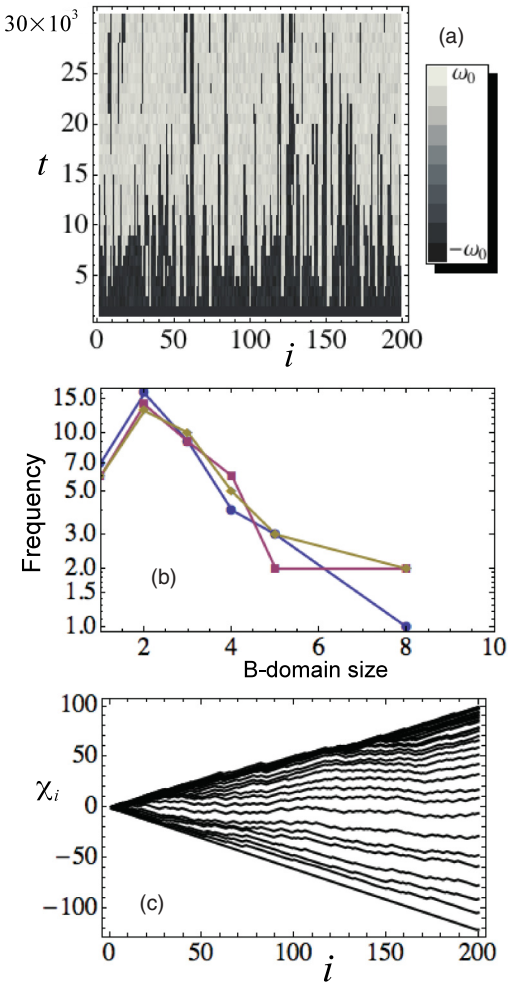

FIG. 2. (Color online) Structural transition dynamics from Z to B form, for $\tau = 0$ and $\kappa = 0.01$. (a) Density plot of ρ_i as functions of dimensionless time t and i. (b) Semilog plot of frequency distributions of B-domain sizes for $t = 799\,000$ (•), 839 000 (■), 879 000(♦) (c) Snapshot graphs of χ_i vs i at dimensionless time $t = 0$, 10^5, $2 \times 10^5, \ldots, 20 \times 10^5$ are plotted from below to top, respectively.

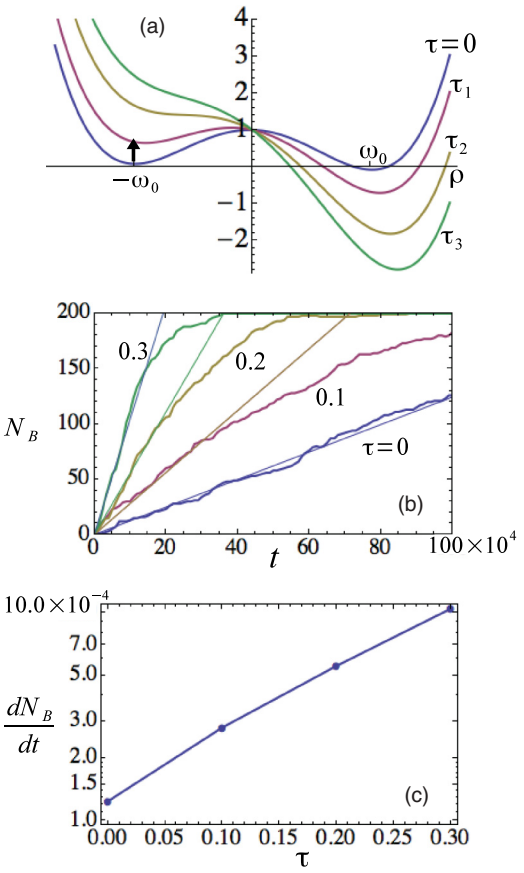

FIG. 3. (Color online) (a) Effective potentials for ρ are plotted for various external torques $\tau = 0$, τ_1, τ_2, τ_3, where $0 < \tau_1 < \tau_2 = 2.65 < \tau_3$. For $\tau = \tau_1$, the activation energy required for transition from Z form to B form is lowered by the amount indicated by the vertical arrow. Larger external torque $\tau = \tau_3$ makes the Z-form structure unstable. τ_2 is the critical value at zero temperature beyond which the Z-form structure is no longer metastable but becomes unstable. (b) Number of B-form segments N_B is plotted as a function of dimensionless time, for $\tau = 0, 0.1, 0.2, 0.3$. Thin lines indicate the linear fitting to the data. (c) The speeds of N_B increases are semilog plotted as a function of τ.

effective potential for structural parameter ρ must be modified by the exerted torque, as depicted in Fig. 3(a). Under a weak external torque τ satisfying $0 < \tau < \tau_2$, the activation energy for transition from Z form to B form is given by

$$\Delta E \simeq \Delta E_0 - \Gamma\tau,$$

where ΔE_0 is the activation energy when $\tau = 0$. Accordingly, nucleation rate p must depend on τ as follows:

$$p \propto \exp(-\beta\Delta E) \propto \exp(\beta\Gamma\tau). \qquad (18)$$

Figure 3(b) plots the total numbers of B-form segments, N_B, as functions of time, for various τ. This figure shows that each N_B initially increases linearly with time, which is consistent with the above confirmed fact that the creations of B-form domains are mediated via statistically uniform nucleation mechanism for weak external torques. From the fitting lines in Fig. 3(b), we obtained the speeds of initial increases, dN_B/dt. Figure 3(c) plots the initial dN_B/dt as a function of τ. This clearly shows the exponential dependency of the nucleation rate to τ, as expressed in Eq. (18).

C. Transition under high external torque

When the external torque exceeds a critical value of $\tau_2 \simeq 2.65$, however, Z-form structure changes from metastable state to unstable state, as shown in Fig. 3(a). Hence, for such high external torque conditions, the structural transition would proceed via a mechanism other than the uniform nucleation.

For the high external torques, the transition dynamics from Z form to B form are shown in Fig. 4(a)–4(c). From Fig. 4(a), we see that the structural transitions occur about 100 times faster than that for the small external torque cases ($\kappa = 0.01$). In particular, the transition is not uniform: It first happens at the terminal on which the external torque is exerted, and then the interface between Z form and B form moves to the other terminal. Due to the B-Z interface-mediated transition, χ_i makes a kink at the interface, as shown in Fig. 4(b). Figure 4(c)

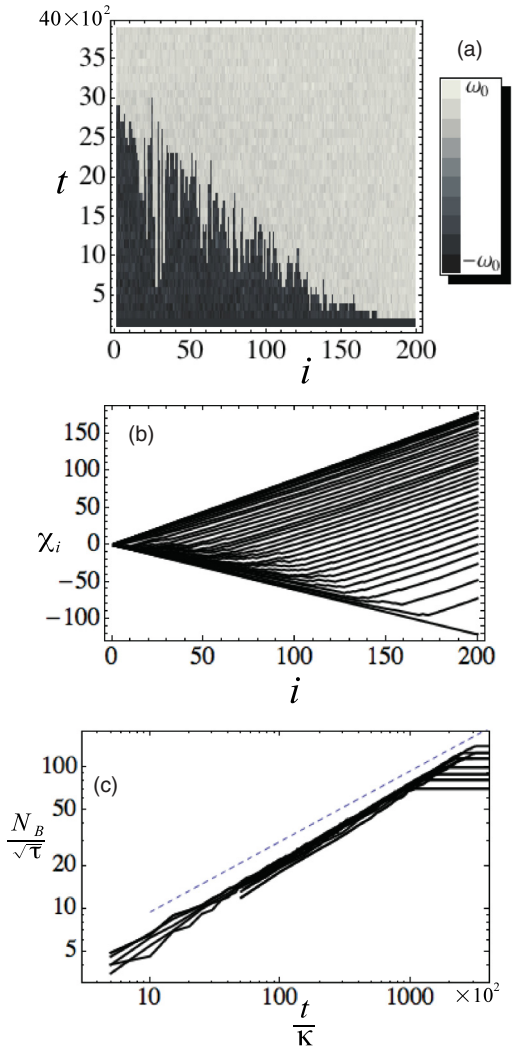

FIG. 4. B-Z transition dynamics under high external torques. (a) Density plot of ρ_i for $\tau = 3$ and $\kappa = 0.01$, as functions of dimensionless time t and i. (b)χ_i vs i for $\tau = 3$ and $\kappa = 0.01$. The curves respectively correspond to $t = 0, 100, 200, \ldots, 2000$ results from below. (c) $N_B/\sqrt{\tau}$ are plotted as functions of t/κ for (τ,κ) in $\tau = 2.5, 3, 4, 5, 6, 8$ and $\kappa = 0.01, 0.1, 1$. All data are scaled onto a master curve. The dashed line $\propto t^{0.5}$ is drawn for eye guidance (see text).

shows the number of B-domain segments N_B as functions of time, where all N_B computed here are fitted well to the following form:

$$\frac{N_B(t)}{\sqrt{\tau}} \propto \left(\frac{t}{\kappa}\right)^{0.5}. \tag{19}$$

This is qualitatively understood from the way of B-form domain growth. Suppose, at a time t, x base pairs from the terminal have already made transitions into a B-form structure. At the moment, the Z-form segment adjacent to the B-Z interface is about to transition into the B form. Let the transition be completed within a time interval $t_{\rm trans}$. Then the sweep speed v of the B-Z interface is given by $1/t_{\rm trans}$. In the following, we will estimate $t_{\rm trans}$. At the beginning of this transition, the angular velocity of the motion is assumed to be zero because of the large viscosity. Moreover, the B-form DNA of length x bp is approximated by a rigid rod of inertia momentum $xI = x(I_1 + I_2)$. Then its angular velocity Ω obeys the following equation:

$$xI\frac{d\Omega}{dt} = \tau - x\kappa\alpha\Omega,$$

resulting in

$$\Omega = \frac{\tau}{x\kappa\alpha}(1 - e^{-\frac{\kappa\alpha}{I}t}).$$

Solving the following equation for $t_{\rm trans}$:

$$2\omega_0 = \int_0^{t_{\rm trans}} \Omega\, dt,$$

one obtains

$$t_{\rm trans} = \sqrt{\frac{4\omega_0 x}{\tau I}} + \frac{\kappa\alpha}{6}\left(\frac{4\omega_0 x}{\tau I}\right) + o[\kappa^2].$$

With this expression, the sweep speed is given by $v = 1/t_{\rm trans}$. Integrating $dx/dt = v = 1/t_{\rm trans}$, we obtain the following relation:

$$\sqrt{\frac{4\omega_0}{\tau I}}x^{3/2} + \frac{\kappa\alpha}{3}\frac{\omega_0 x^2}{\tau I} = t.$$

For large x, we have

$$\frac{x}{\sqrt{\tau I}} \sim \left(\frac{t}{\kappa\alpha}\right)^{1/2},$$

and therefore Eq. (19) holds.

We have confirmed that the unstable segment adjacent to the B-Z interface induces the structural transition dynamics. Hence, the transition dynamics can be called a kind of real-space spinodal decomposition, in contrast to the usual spionodal decomposition that occurs in reciprocal space.

V. CONCLUSION

In this paper, we studied the dynamics of a linear DNA molecule. To this end, the statistical model given in Ref. [12] is generalized by including rotational kinetic energies. Then the dynamics under the external torque in a surrounding physiological buffer is modeled by a Langevin equation.

In Sec. IV A, by using the Langevin dynamics, we first simulated the relaxation phenomena after sudden additions of external torques. We found that the total kinetic energy shows nonexponential slow relaxation as $K = Bt^{-1/2}$, which is a characteristic of one-dimensional nonlinear dynamical systems. In contrast, K relaxes exponentially with t for the linearized equations of motions, which means that the nonlinearity is indispensable for the nonexponential decay. The prefactor B turned out to depend on viscosity proportional constant κ, as $B \sim \kappa^{-3/2}$. We found that this can be qualitatively understood from the fact that the dynamics of nonconservative systems depart from the behavior of the conserved system at the relaxation times of $t_{\rm relax} \sim 1/\kappa$.

We then proceeded to study the dynamics of structural transition from Z form to B form under external torques, τ, exerted on a terminal (Sec. IV B). For small external torques, B-form domains nucleate and grow. This statistical process occurs uniformly within the whole DNA segments. The speed

of B-domain growth thus obeys an Arrhenius equation with the activation energy $\Delta E = \Delta E_0 - \Gamma\tau$, where ΔE_0 is the activation energy for $\tau = 0$ and Γ is the linear response coefficient of the activation energy to the external torque τ.

In contrast to this, when the external torque is larger than a critical value, Z-form structure becomes unstable rather than metastable. For such a high external force, the transition mechanism is switched to a spatially inhomogeneous spinodal-like process (Sec. IV C). Namely, the transition first occurs at the terminal which the external torque acts on. Then the B-Z interface created there starts to sweep to the other terminal. When the interface reaches the other terminal, the whole transition is completed. In this case the number of B-form segments scales as $\propto t^{1/2}$ with time t. We gave a phenomenological estimate that accounts for this numerically obtained scaling, in which we assumed that the B-form DNA is approximated by a rigid rod and that the transition into B form, occurring at the Z-form segment adjacent to the B-Z interface, gives rise to the rotation of the B-form rod. Using these two assumptions, we reproduced the numerically obtained scaling relation as $x/\sqrt{\tau I} \sim (t/\kappa\alpha)^{1/2}$.

We expect that the simple dynamical model developed in this paper equips the essence of interaction between DNA chiral structure and the mechanical response to the external forces, and hence we believe that the various structural transition phenomena elucidated in this paper can be verified in future experiments.

It is noteworthy to remark that we have neglected the hydrodynamic interaction between DNA segments in modeling the effect of physiological buffer, as discussed in Sec. II. This effect would become important especially for studying dynamical interaction between structures (e.g., B form, Z form) and three-dimensional configurations (e.g., plectoneme) of a DNA molecule, because two segments, far apart from each other in a nucleic acid sequence, can be spatially close to each other. The inclusion of this effect is a further task of this work.

As a final remark, we note that the dynamical aspects we have developed will provide a useful tool for investigating the dynamics of other structural transitions, such as a denaturation process [18,20,21].

APPENDIX: KINK PROPAGATION IN A CONSERVED SYSTEM

In this Appendix, we show that kink propagations occur in the conserved system (i.e, $T = 0, \kappa = 0$). As an ideal case, we consider a DNA molecule of infinite length without external torques. From the principle of least action, we derive equations of motions for $\Theta(s,t)$ and $\chi(s,t)$. The action is given by $S = \int_0^t L\, dt$, where L is the Lagrangian of Eq. (3). The first variation of S is given by

$$\delta S = \iint \left[\left\{ -I_1 \frac{\partial^2\Theta}{\partial t^2} - C\frac{\partial^2}{\partial s^2}(\chi - \Theta) - d_1\frac{\partial^4\Theta}{\partial s^4} + \frac{\partial}{\partial s}\left(\frac{\partial \mathcal{V}}{\partial \rho}\right) \right\}\delta\Theta + \left\{ -I_2\frac{\partial^2\chi}{\partial t^2} + C\frac{\partial^2}{\partial s^2}(\chi - \Theta) \right\}\delta\chi \right] ds\, dt. \quad \text{(A1)}$$

Arbitrary $\delta\chi$ and $\delta\Theta$ should satisfy $\delta S = 0$, which gives the following equations of motion:

$$-I_1\frac{\partial^2\Theta}{\partial t^2} - C\frac{\partial^2}{\partial s^2}(\chi - \Theta) - d_1\frac{\partial^4\Theta}{\partial s^4} + \frac{\partial}{\partial s}\left(\frac{\partial \mathcal{V}}{\partial \rho}\right) = 0, \quad \text{(A2)}$$

$$-I_2\frac{\partial^2\chi}{\partial t^2} + C\frac{\partial^2}{\partial s^2}(\chi - \Theta) = 0. \quad \text{(A3)}$$

To obtain kink solutions with velocities v, we set

$$\chi(s,t) = F(s - vt), \quad \Theta(s,t) = G(s - vt)$$

in Eqs. (A2) and (A3). Thereby, these equations reduce to the following ordinary differential equations for $F(x)$ and $G(x)$ with $x = s - vt$:

$$-I_1 v^2\frac{d^2G}{dx^2} - C\frac{d^2}{dx^2}(F - G) - d_1\frac{d^4G}{dx^4} + \frac{d}{dx}\left(\frac{d\mathcal{V}}{d\rho}\right) = 0, \quad \text{(A4)}$$

$$-I_2 v^2\frac{d^2F}{dx^2} + C\frac{d^2}{dx^2}(F - G) = 0. \quad \text{(A5)}$$

By eliminating F from these equations, the equation for G is given by

$$d_1\frac{d^4G}{dx^4} + A\frac{d^2G}{dx^2} - \frac{d}{dx}\left(\frac{d\mathcal{V}}{d\rho}\right) = 0$$

with

$$A = I_1 v^2 + \frac{I_2 v^2 C}{C - I_2 v^2}. \quad \text{(A6)}$$

This equation gives a first integral

$$d_1\frac{d^3G}{dx^3} + A\frac{dG}{dx} - \frac{d\mathcal{V}}{d\rho} = C_1.$$

By setting $g(x) = \frac{dG(x)}{dx}$, one obtains

$$d_1\frac{d^2g}{dx^2} + Ag - \frac{\partial\mathcal{V}}{\partial\rho}(g) = C_1.$$

This is the equation of motion for a particle of mass d_1 moving in a potential of $\frac{A}{2}g^2 - \mathcal{V}(g) - C_1 g$. Hence, we obtain the following another first integral:

$$C_2 = \frac{d_1}{2}\left(\frac{dg}{dx}\right)^2 + \frac{A}{2}g^2 - \mathcal{V}(g) - C_1 g. \quad \text{(A7)}$$

According to Jensen *et al.* [15,22], here we assume the following symmetric potential $\mathcal{V}(\rho) = \mathcal{V}_0[(\rho/\omega_2)^2 - 1)]^2$. For Eq. (A7) to allow for kink solutions, we have to choose C_1 and C_2 as follows:

$$C_1 = 0, \quad C_2 = \frac{\omega_0^4}{\mathcal{V}_0}\left(\frac{\mathcal{V}_0}{\omega_0^2} + \frac{A}{4}\right)^2 - \mathcal{V}_0.$$

The resulting equation is given by

$$\left(\frac{dg}{dX}\right)^2 = (g^2 - a^2)^2, \quad \text{(A8)}$$

where $a^2 = \omega_0^2 + \frac{\omega_0^4 A}{2\mathcal{V}_0}$ and $X = x/\sqrt{d_1\omega_0^4/2\mathcal{V}_0}$. This equation has kink solutions $g(X) = \pm a\tanh(aX)$.

Note here that the family of kink solutions exist for arbitrary v with $v^2 < C/I_2$ [see Eq. (A6)], which is in contrast to the result of nonconservative systems, where the speeds of interfaces were uniquely determined with the viscosity (Sec. IV C).

[1] C. Bustamante, Z. Bryant, and S. B. Smith, Nature (London) **421**, 423 (2003).
[2] Z. Bryant, M. D. Stone, J. Gore, S. B. Smith, N. R. Cozzarelli, and C. Bustamante, Nature (London) **424**, 338 (2003).
[3] T. Strick, J. Allemand, V. Croquette, and D. Bensimon, Prog. Biophys. Mol. Biol. **74**, 115 (2000); T. R. Strick, J. F. Allemand, D. Bensimon, A. Bensimon, and V. Croquette, Science **271**, 1835 (1996).
[4] J. F. Marko, in *Multiple Aspects of DNA and RNA: From Biophysics to Bioinformatics*, Les Houches 2004, edited by D. Chatenay *et al*. (Elsevier, Amsterdam, 2005).
[5] J. F. Marko and E. D. Siggia, Science **265**, 506 (1994); Phys. Rev. E **52**, 2912 (1995); C. Bouchiat and M. Mézard, Phys. Rev. Lett. **80**, 1556 (1998); B. Fain and J. Rudnick, Phys. Rev. E **60**, 7239 (1999).
[6] B. C. Daniels, S. Forth, M. Y. Sheinin, M. D. Wang, and J. P. Sethna, Phys. Rev. E **80**, 040901(R) (2009).
[7] T. B. Liverpool, S. A. Harris, and C. A. Laughton, Phys. Rev. Lett. **100**, 238103 (2008).
[8] R. D. Kamien, T. C. Lubensky, P. Nelson, and C. S. O'Hern, Europhys. Lett. **38**, 237 (1997); P. Nelson, Biophys. J. **74**, 2501 (1998); J. D. Moroz and P. Nelson, Macromolecules **31**, 6333 (1998).
[9] J. F. Léger, G. Romano, A. Sarkar, J. Robert, L. Bourdieu, D. Chatenay, and J. F. Marko, Phys. Rev. Lett. **83**, 1066 (1999); A. Sarkar, J. F. Léger, D. Chatenay, and J. F. Marko, Phys. Rev. E **63**, 051903 (2001).
[10] J. Yan and J. F. Marko, Phys. Rev. Lett. **93**, 108108 (2004).
[11] J. Palmeri, M. Manghi, and N. Destainville, Phys. Rev. Lett. **99**, 088103 (2007); M. Manghi, J. Palmeri, and N. Destainville, J. Phys.: Condens. Matter **21**, 034104 (2009).
[12] T. Okushima and H. Kuratsuji, Phys. Rev. E **84**, 021926 (2011).
[13] M. Lee, S. H. Kim, and S.-C. Hong, Proc. Natl. Acad. Sci. USA **107**, 4985 (2010).
[14] For example, G. Wang, S. Carbajal, J. Vijg, J. DiGiovanni, and K. M. Vasquez, J. Natl. Cancer Inst. **100**, 1815 (2008).
[15] P. Jensen, Marko V. Jarić, and K. H. Bennemann, Phys. Lett. A **95**, 204 (1983).
[16] J. F. Marko, Phys. Rev. E **76**, 021926 (2007).
[17] S. N. Volkov, J. Theor. Biol. **143**, 485 (1990). In the paper, a similar model is developed to describe the B- to A-form transition.
[18] See, e.g., L. V. Yakushevich, *Nonlinear Physics of DNA*, 2nd ed. (Wiley-VCH, Boschstrasse, Weinheim, Germany, 2004).
[19] G. P. Tsironis and S. Aubry, Phys. Rev. Lett. **77**, 5225 (1996).
[20] M. Peyrard and A. R. Bishop, Phys. Rev. Lett. **62**, 2755 (1989); T. Dauxois, M. Peyrard, and A. R. Bishop, Phys. Rev. E **47**, 684 (1993).
[21] S. Cocco and R. Monasson, Phys. Rev. Lett. **83**, 5178 (1999).
[22] The relative depths of minima depend on the salt concentration as shown in Refs. [13,15].